Original Article

Institution of MECHANICAL ENGINEERS
Journal of MECHANICAL ENGINEERING SCIENCE

Proc IMechE Part C:
J Mechanical Engineering Science
227(11) 2549–2562

DOI: 10.1177/0954406213475980
pic.sagepub.com
SAGE

# Design of an Ackermann-type steering mechanism

**Jing-Shan Zhao[1], Xiang Liu[1], Zhi-Jing Feng[1] and Jian S Dai[2,3]**

**Abstract**

This article focuses on the synthesis of a steering mechanism that exactly meets the requirements of Ackermann steering geometry. It starts from reviewing of the four-bar linkage, then discusses the number of points that a common four-bar linkage could precisely trace at most. After pointing out the limits of a four-bar steering mechanism, this article investigates the turning geometry for steering wheels and proposes a steering mechanism with incomplete noncircular gears for vehicle by transforming the Ackermann criteria into the mechanism synthesis. The pitch curves, addendum curves, dedendum curves, tooth profiles and transition curves of the noncircular gears are formulated and designed. Kinematic simulations are executed to demonstrate the target of design.

**Keywords**

Ackermann criteria, steering mechanism, four-bar linkage, noncircular gears

Date received: 14 August 2012; accepted: 7 January 2013

## Introduction

The generally used steering mechanisms for four-wheel vehicles are four-bar linkages[1,2] which are often called Ackermann-type steering mechanisms.[1–6] The input motion from the driver at the steering wheel is transmitted via a steering box and the steering control linkage to one of the steering knuckles and then transmitted to the other one through the Ackermann steering linkage.[6] The main kinematic requirement of the steering linkage of a vehicle is to provide the steerable wheels a correlated pivot such that their axes intersect at a point on the rear wheel axis.[7] The objective for the synthesis of steering mechanism is to minimise the difference between the steering centres over the full range of steering angle inputs while fitting into a reasonable space.[8] To obtain the target, several conflicting requirements should be simultaneously considered.[5] A possible formulation of the optimisation-based synthesis problem is to search for the values of parameters.[7]

Most trucks and off-highway vehicles have rigid steering axles equipped with Ackermann steering linkage.[6] So synthesis of function generators is a common mechanism design problem for steering systems of vehicles. The deviation between the desired and the real pivoting angles given to the wheels by the steering mechanism is called steering error.[7] It requires finding the geometric parameters for which the input–output relationship of the mechanism best approximates a specified function.[4,9] Error optimisation studies in steering linkages have been attempted by many researchers.[10] The primary goals are ensuring minimum wheel-slip and symmetric steering control for left and right turns, ensuring minimum cross-coupling between steering and axle oscillation, maintaining favorable pressure angles in the joints, and avoiding interference between the moving parts of the mechanism and between them and the body of the vehicle.[5]

For the purpose of improving maneuverability at low speed and controllability and stability at high speed,[11] a general method of optimal synthesis of steering mechanisms is developed by displacement matrix and constraints.[3] Design charts are presented which considerably facilitates the work of engineers in

[1]State Key Laboratory of Tribology, Department of Mechanical Engineering, Tsinghua University, Beijing, PR China
[2]Centre for Advanced Mechanisms and Robotics, Tianjin University, Tianjin, PR China
[3]King's College London, University of London, London, UK

**Corresponding author:**
Jing-Shan Zhao, State Key Laboratory of Tribology, Department of Mechanical Engineering, Tsinghua University, Beijing 100084, PR China.
Email: jingshanzhao@mail.tsinghua.edu.cn

determining the optimum geometry of the central-lever steering mechanism of a vehicle.[7] Also, the minimum of the maximum steering errors of the steering linkage are considered as one of the optimisation targets.[8] The sensitivity analysis is investigated with the design charts on which how parametric errors affect the performance of the steering mechanism.[12] A kinematic model of a rack-and-pinion-type steering linkage is developed, on the basis of which the synthesis of the mechanism is performed using the criteria of correct turning of the wheels and good transmissibility of the motion.[13] The practical cases of the rack-and-pinion and central-lever steering linkages are examined as planar mechanisms, and a maximum number of only three and four independent design parameters, respectively, are proven to exist.[14] A vehicle model is developed employing a detailed nonlinear kinematic representation of a MacPherson strut front independent automotive suspension with a rack and pinion steering system.[15] In the kinematic study of the McPherson-type steering suspension, the departure in the suspension geometry is expressed as a function of the travel of the strut and of the turn of the steering wheel.[16]

In addition, differential mechanism coupled to a higher pair, resolves the single input coming from the steering wheel into two outputs satisfying the condition of correct steering.[17] Structure classification, number and dimensional synthesis of independent suspension mechanisms were investigated through the atlas of in-parallel suspension linkages.[18] Similarly the steering mechanism, which is often proposed as planar linkages,[4,10,19] can be synthesised to satisfy the needs of number and size in engineering. However, the synthesis of a steering mechanism that meets the requirements of Ackermann turning geometry is far more complicated than the structure only. It is an exact trajectory tracing mechanism. Therefore, the Ackermann criteria should be put into the dimension synthesis of the steering mechanism. Noncircular gears make it possible to synthesise a steering mechanism that satisfies the Ackerman criteria.[20,21] However, the new steering mechanism[20] and the eight-link mechanism[21] are much more complicated than the traditional four-bar steering systems.

This article starts from the discussion of the number of points that a planar four-bar linkage could precisely trace, and then proposes a noncircular gear coupled steering mechanism which could strictly follow the Ackermann steering rule compared with the existing four-bar steering linkages.

## Restrictions of a four-bar steering linkage

The existing mechanical steering systems used in the automobiles all belong to four-bar linkages. To comprehensively understand the characteristics of the four-bar steering mechanism, the ideal turning criteria for a vehicle should be first discussed.

### Ackermann criteria for turning wheels

Figure 1 illustrates the ideal geometry conditions for an automobile to turn right when the four wheels only make pure rotations about an instant centre $o$.

This geometry requirement shown in Figure 1 can be expressed as

$$l\cot\theta_1 - l\cot\theta_2 = b \tag{1}$$

where $l$ denotes the wheelbase, $b$ represents the track of front wheels, $\theta_1$ and $\theta_2$ indicate the due angles of the front left and front right wheels.

Rearranging equation (1) presents

$$\cot\theta_1 - \cot\theta_2 = \frac{b}{l} \tag{2}$$

Equation (2) is called the ideal Ackermann turning criteria.[2,7,10] Suppose that the turning angles shown in Figure 1 are the upper limits when turning right. To keep the front wheels always satisfying this ideal constraint, the instant centres of the four wheels will shift from point $o$ to infinity.

However, if the turning angles do not satisfy to the Ackermann turning criteria, the rotation centres of left front wheel and right front wheel will do not coincide with each other. In this condition, the wheels are not only rotating but also sliding. Hence, the steering error can significantly affect the tire wear especially in high speed.[22] As a result, a steering mechanism meeting the requirements of Ackermann turning criteria is very meaningful in applications.

Could the steering four-bar linkage meet the needs of ideal Ackermann turning criteria? What follows will first discuss the maximal number of points that a general planar four-bar linkage could exactly trace.

### The maximum number of points a planar four-bar linkage could trace

Suppose that there is a planar four-bar mechanism shown in Figure 2. Its end-effector is triangle $BCE$.

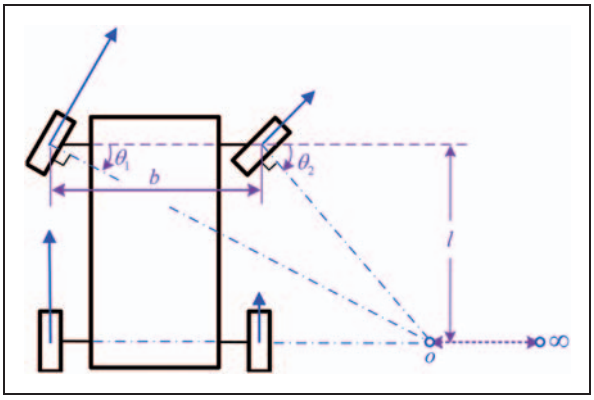


**Figure 1.** Ideal Ackermann turning geometry.

In the planar four-bar mechanism system shown in Figure 2, there are 9 independent variables, namely $x, y, \theta$ and $s_i (i = 1, 2, \ldots, 6)$. Now, a pair of variables $\varphi_{1i}$ and $\varphi_{2i}$ are introduced for a specified point $E_j (j = 1, 2, \ldots)$. In the coordinate frame $x_1 A y_1$, the coordinates of the four joints are

$$\begin{aligned} \boldsymbol{r}_{A_1} &= \begin{bmatrix} 0 \\ 0 \end{bmatrix}, \ \boldsymbol{r}_{B_1} = s_1 \begin{bmatrix} \cos\varphi_1 \\ \sin\varphi_1 \end{bmatrix}, \\ \boldsymbol{r}_{C_1} &= \begin{bmatrix} s_4 + s_3\cos\varphi_2 \\ s_3\sin\varphi_2 \end{bmatrix}, \ \boldsymbol{r}_{D_1} = \begin{bmatrix} s_4 \\ 0 \end{bmatrix} \end{aligned} \tag{3}$$

The absolute coordinates of these four joints can be expressed as

$$\boldsymbol{r}_X = \boldsymbol{r}_A + \mathbf{R}\boldsymbol{r}_{X_1} \tag{4}$$

where $X = A, B, C, D$ and therefore $\boldsymbol{r}_{X_1}$ represents the vectors in equation (3), $\boldsymbol{r}_A = \begin{bmatrix} x \\ y \end{bmatrix}$ and $\mathbf{R} = \begin{bmatrix} \cos\theta & -\sin\theta \\ \sin\theta & \cos\theta \end{bmatrix}$.

Substituting equations (3) in equation (4), one obtains

$$\begin{aligned} \boldsymbol{r}_A &= \begin{bmatrix} x \\ y \end{bmatrix}, \ \boldsymbol{r}_B = \begin{bmatrix} x + s_1\cos(\varphi_1 + \theta) \\ y + s_1\sin(\varphi_1 + \theta) \end{bmatrix}, \\ \boldsymbol{r}_C &= \begin{bmatrix} x + s_4\cos\theta + s_3\cos(\varphi_2 + \theta) \\ y + s_4\sin\theta + s_3\sin(\varphi_2 + \theta) \end{bmatrix}, \\ \boldsymbol{r}_D &= \begin{bmatrix} x + s_4\cos\theta \\ s_4\sin\theta \end{bmatrix} \end{aligned} \tag{5}$$

For $E_j (j = 1, 2, \ldots)$ are known points, one can assume that

$$\boldsymbol{r}_{E_j} = \begin{bmatrix} x_j & y_j \end{bmatrix}^T \tag{6}$$

The following equations will always hold:

$$\begin{cases} |\boldsymbol{r}_C - \boldsymbol{r}_B| = s_2 \\ |\boldsymbol{r}_{E_i} - \boldsymbol{r}_B| = s_5 \\ |\boldsymbol{r}_{E_i} - \boldsymbol{r}_C| = s_6 \end{cases} \tag{7}$$

Therefore, one additional independent equation should be provided whenever a new point $E_i$ is introduced into the constraint system besides the pair of variables $\varphi_1$ and $\varphi_2$ correspondingly. As a result, the 9 independent variables need and only need 9 different points. So a planar four-bar linkage can only precisely trace 9 points. In other words, the trapezoid steering four-bar mechanism cannot always follow the Ackermann criteria from point $o$ to infinity. Therefore, the existing mechanical steering mechanisms could not always satisfy the Ackermann criteria when steering. Although the deformations resulting from the elastic links and rubber bushing could modify the Ackermann function, the method to synthesise such function-driven mechanism is urgently necessary in engineering applications and mechanism theory.

## Ackermann-type steering mechanism

This section focuses on the synthesis of Ackermann steering geometry and proposes a steering mechanism that could satisfy the ideal turning requirements.

### *Requirements for an Ackermann-type steering mechanism*

Suppose the bottom angle of a trapezoid linkage $ABCD$ shown in Figure 3, is denoted by $\psi$, then when the turning angle equals to zero, the initial length of link $BC$, $l_{20}$, can be expressed as

$$l_{20} = l_4 - 2l_1\cos\psi \tag{8}$$

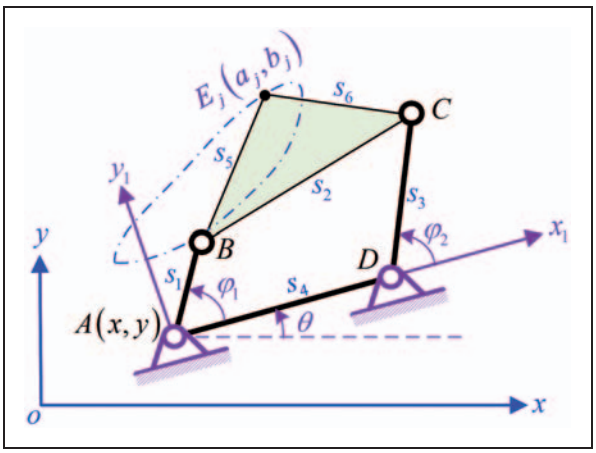


**Figure 2.** Trace of a four-bar linkage.

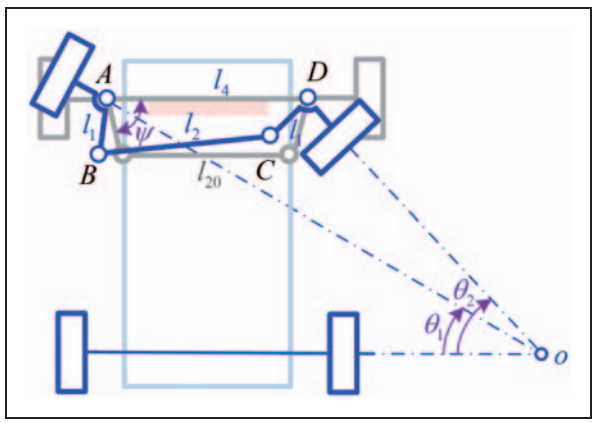


**Figure 3.** Ideal steering mechanism for Ackermann turning geometry.

The steering linkage that meets the needs of Ackermann turning geometry is a particular path tracing mechanism. During turning right, the left wheel turned $\theta_1$ and the right wheel turned $\theta_2$ correspondingly. To satisfy the Ackermann turning geometry, the length of the link should be

$$\begin{aligned} l_2 &= \sqrt{\left[l_4 - l_1\cos(\psi-\theta_2) - l_1\cos(\psi+\theta_1)\right]^2 + \left[l_1\sin(\psi-\theta_2) - l_1\sin(\psi+\theta_1)\right]^2} \\ &= \sqrt{2l_1^2 + l_4^2 + 2l_1^2\cos(2\psi+\theta_1-\theta_2) - 2l_1l_4[\cos(\psi-\theta_2)+\cos(\psi+\theta_1)]} \end{aligned} \tag{9}$$

where $l_2$ represent the length of link $BC$ that satisfies the Ackermann turning criteria.

From equation (2), one obtains

$$\theta_2 = \operatorname{arc\,cot}\left(\cot\theta_1 - \frac{b}{l}\right) \tag{10}$$

Substituting equation (10) into equation (9) yields

$$l_2 = l_4\sqrt{1+2\xi^2+2\xi^2\cos[2\psi+\theta_1-\operatorname{arc\,cot}(\cot\theta_1-\varsigma)] - 2\xi\left\{\cos(\psi+\theta_1)+\cos[\psi-\operatorname{arc\,cot}(\cot\theta_1-\varsigma)]\right\}} \tag{11}$$

where $\xi = \frac{l_1}{l_4}$, $\varsigma = \frac{b}{l}$.

Equation (11) indicates that the length of the link, $l_2$, should change with the change of the turning angle, $\theta_1$, if the Ackermann criteria were satisfied.

## Synthesis of the Ackermann-type steering mechanism

Suppose the original fixed link $BC$ are replaced by an Assur II-group linkage[23] $BEC$ shown in Figure 4. It is an RRR-group linkage. Simultaneously, the link $BE$ is welded with a noncircular incomplete gear which meshes another noncircular incomplete gear fixed with the chassis. So, the synthesis of the steering mechanism is now transformed into the design of a pair of noncircular gears and an Assur II-group of revolute jointed linkage $BEC$ shown in the circled section of Figure 4 to satisfy equation (11). The link $BE$ and $EC$ keep in one horizontal line at the position of zero turning which is shown by the gray lines in Figure 4.

Suppose that the length of link $BE$ is represented by $u$ and the length of link $EC$ is represented by $v$. The detailed structure of the geared five-bar steering mechanism is shown in Figure 5. In this figure, $\omega$ is the angular velocity of link $AB$, $\omega_{r1}$ is the relative angular velocity of noncircular gear 1 with respect to link $AB$, $\omega_{r2}$ is the relative angular velocity of noncircular gear 2 with respect to link $AB$, $\beta$ is the angle between $AB$ and $BC$, $\gamma$ is the angle between $BC$ and $BE$. Assume that the vehicle is turning from left to right, then the angular velocity directions of $\omega_{r1}$ and $\omega_{r2}$ are shown in Figure 5.

The coordinates of joints, $A$, $B$ and $C$, in the coordinate system $x_1o_1y_1$ are

$$\begin{cases} A(0 \quad 0) \\ B(l_1\cos(\psi+\theta_1) \quad -l_1\sin(\psi+\theta_1)) \\ C(l_4 - l_1\cos(\psi-\theta_2) \quad -l_1\sin(\psi-\theta_2)) \end{cases} \tag{12}$$

So the angle $\beta$ is indicated by

$$\begin{aligned} \beta &= \arccos\left(\frac{\overrightarrow{BA}\cdot\overrightarrow{BC}}{||\overrightarrow{BA}||\,||\overrightarrow{BC}||}\right) \\ &= \arccos\left\{\frac{l_1[1+\cos(2\psi+\theta_1-\theta_2)] - l_4\cos(\psi+\theta_1)}{l_2}\right\} \end{aligned} \tag{13}$$

where $\overrightarrow{BA}$ stands for a vector from point $B$ to point $A$, '$\cdot$' indicates the inner product of two vectors, and $||\overrightarrow{BA}||$ represents the Euclidean norm of vector $\overrightarrow{BA}$. In addition, the angle $\beta$ is always in the interval of $[0,\pi]$ considering the actual steering situations. Because arc $\cos(x)$ is monotonic and real within the interval of $[0,\pi]$ in accordance with the definition of the inverse cosine, equation (13) has a unique solution.

Substituting equation (11) into equation (13) yields

$$\beta = \operatorname{arc\ cos}\left(\frac{\xi\left\{1+\cos[2\psi+\theta_1-\operatorname{arc\,cot}(\cot\theta_1-\varsigma)]\right\} - \cos(\psi+\theta_1)}{\sqrt{1+2\xi^2+2\xi^2\cos[2\psi+\theta_1-\operatorname{arc\,cot}(\cot\theta_1-\varsigma)] - 2\xi\left\{\cos(\psi+\theta_1)+\cos[\psi-\operatorname{arc\,cot}(\cot\theta_1-\varsigma)]\right\}}}\right) \tag{14}$$

At the zero turning position, one obtains

$$v = l_{20} - u \tag{15}$$

So the angle $\gamma$ is represented by

$$\gamma = \operatorname{arc\ cos}\left(\frac{u^2+l_2^2-v^2}{2ul_2}\right) = \operatorname{arc\ cos}\left(\frac{l_2^2-l_{20}^2+2ul_{20}}{2ul_2}\right) \tag{16}$$

Similarly, because the angle $\gamma$ is also defined within the interval of $[0, \pi]$, equation (16) has one solution.

Then the relative rotational angle between $\overrightarrow{BA}$ and $\overrightarrow{BE}$, $\phi$, is

$$\begin{cases} \phi = \beta + \gamma + \psi - \pi, & \theta_1 \geqslant 0 \\ \phi = \beta - \gamma + \psi - \pi, & \theta_1 < 0 \end{cases} \tag{17}$$

where $\theta_1 \geqslant 0$ indicates that the vehicle turns right, vice versa, $\theta_1 < 0$ indicates that the vehicle turns left.

The relative angular velocity of link $BE$ with respect to link $BA$ is indicated by

$$\omega_{r2} = \frac{\mathrm{d}\phi}{dt} \tag{18}$$

The absolute angular velocity of link $BA$ is

$$\omega = \frac{\mathrm{d}\theta_1}{dt} \tag{19}$$

Because the fact that gear 1 is fixed with the chassis, the relative angular velocity of noncircular gear 1 is

$$\omega_{r1} = -\omega \tag{20}$$

The relative transmission ratio of noncircular gears 1 and 2 with respect to link $AB$ is

$$i^r_{21} = \frac{\omega_{r2}}{\omega_{r1}} = \frac{\dfrac{\mathrm{d}\phi}{dt}}{-\dfrac{\mathrm{d}\theta_1}{dt}} = -\frac{\mathrm{d}\phi}{d\theta_1} = \begin{cases} -\left(\dfrac{\mathrm{d}\beta}{d\theta_1} + \dfrac{\mathrm{d}\gamma}{d\theta_1}\right), & \theta_1 \geqslant 0 \\ -\left(\dfrac{\mathrm{d}\beta}{d\theta_1} - \dfrac{\mathrm{d}\gamma}{d\theta_1}\right), & \theta_1 < 0 \end{cases} \tag{21}$$

where '$-$' represents that the rotations of noncircular gear 1 and noncircular gear 2 are in opposite directions.

$\frac{\mathrm{d}\beta}{d\theta_1}$ and $\frac{\mathrm{d}\gamma}{d\theta_1}$ can be obtained from equations (13) and (16), respectively

$$\frac{\mathrm{d}\beta}{d\theta_1} = \frac{l_1 l_2 (1-\sigma_1)\sin[2\psi + \theta_1 - \operatorname{arc\,cot}(\cot\theta_1 - \varsigma)] - l_2 l_4 \sin(\psi + \theta_1) + \sigma_2 \dfrac{\mathrm{d}l_2}{d\theta_1}}{l_2\sqrt{l_2^2 - \sigma_2^2}} \tag{22}$$

where $\sigma_1 = \frac{\mathrm{d}\theta_2}{d\theta_1} = \frac{1}{(\cos\theta_1 - \varsigma\sin\theta_1)^2 + \sin^2\theta_1}$, $\sigma_2 = l_1\{1 + \cos[2\psi + \theta_1 - \operatorname{arc\,cot}(\cot\theta_1 - \varsigma)]\} - l_4\cos(\psi + \theta_1)$,

$$\frac{\mathrm{d}l_2}{d\theta_1} = \frac{l_4\xi\left\{\sin(\psi + \theta_1) - \sigma_1\sin[\psi - \operatorname{arc\,cot}(\cot\theta_1 - \varsigma)] - \xi(1-\sigma_1)\sin[2\psi + \theta_1 - \operatorname{arc\,cot}(\cot\theta_1 - \varsigma)]\right\}}{\sqrt{1 + 2\xi^2 + 2\xi^2\cos[2\psi + \theta_1 - \operatorname{arc\,cot}(\cot\theta_1 - \varsigma)] - 2\xi\left\{\cos(\psi + \theta_1) + \cos[\psi - \operatorname{arc\,cot}(\cot\theta_1 - \varsigma)]\right\}}}$$

And

$$\frac{\mathrm{d}\gamma}{d\theta_1} = -\frac{\left(l_2^2 + l_{20}^2 - 2ul_2\right)\frac{\mathrm{d}l_2}{d\theta_1}}{l_2\sqrt{4u^2 l_2^2 - \left(l_2^2 - l_{20}^2 + 2ul_{20}\right)^2}} \tag{23}$$

$i^r_{21}$ can also be expressed as

$$i^r_{21} = -\frac{r_1}{r_2} \tag{24}$$

where '$-$' represents that noncircular gear 1 rotates in an opposite direction as noncircular gear 2 does and

$$r_1 + r_2 = l_1 \tag{25}$$

From equations (24) and (25), one can find that

$$\begin{cases} r_1 = -\frac{i^r_{21} l_1}{1 - i^r_{21}} \\ r_2 = \frac{l_1}{1 - i^r_{21}} \end{cases} \tag{26}$$

Equation (26) represents the pitch curves of the noncircular incomplete gears used to remedy the errors resulting from the fixed length of the link, denoted by $l_{20}$ in Figure 3, which is used in the traditional trapezoid steering linkages. According to equation (22) and equation (23), one obtains that $\frac{\mathrm{d}\beta}{d\theta_1}$ and $\frac{\mathrm{d}\gamma}{d\theta_1}$ are continuous about $\theta_1$, $\lim_{\theta_1 \to 0} \frac{\mathrm{d}\gamma}{d\theta_1} = 0$ and $\lim_{\theta_1 \to 0} \frac{\mathrm{d}^2\gamma}{d\theta_1^2} = 0$, so $i^r_{21}$ is continuous about $\theta_1$, then the functions of the pitch curves expressed by equation (26) are continuous about $\theta_1$.

## Sensitivity analysis

Without a doubt, the manufacturing errors and wears in joints, which are unavoidable in applications, could affect the accuracy of the mechanism. Hence, the sensitivity analysis is absolutely essential to the design.

Assuming that the transmission ratio of the noncircular gear pair is specified as $i^r_{21}$ which satisfies the Ackermann steering criteria. It is a continuous function about the steering angle, $\theta_1$. The relative rotational angle between $\overrightarrow{BA}$ and $\overrightarrow{BE}$, denoted by $\phi$, can be expressed as

$$\phi = \begin{cases} \int_0^{\theta_1} i^r_{21}\mathrm{d}\vartheta & \theta_1 \geqslant 0 \\ -\int_{\theta_1}^{0} i^r_{21}\mathrm{d}\vartheta & \theta_1 < 0 \end{cases}$$

where $\theta_1 \geqslant 0$ indicates that the vehicle turns right, vice versa, $\theta_1 < 0$ indicates that the vehicle turns left.

Accordingly, the subtended angle between $\overrightarrow{BA}$ and $\overrightarrow{BE}$ is

$$\varphi = \pi - \psi + \phi$$

The coordinates of joint $E$ in coordinate system $x_1o_1y_1$ shown in Figure 5 are

$$\begin{cases} x_E = u\cos(\theta_1 + \phi) + l_1\cos(\psi + \theta_1) \\ y_E = -u\sin(\theta_1 + \phi) - l_1\sin(\psi + \theta_1) \end{cases} \quad (27)$$

Point $C$ is on the circle whose centre is point $D$ and radius is $l_1$. Hence,

$$\begin{cases} x_C = l_4 - l_1\cos(\psi - \theta_2) \\ y_C = -l_1\sin(\psi - \theta_2) \end{cases} \quad (28)$$

Then the relationship between point $C$ and $E$ is

$$(x_E - x_C)^2 + (y_E - y_C)^2 = v^2 \quad (29)$$

Substituting equations (27) and (28) into equation (29) presents the relationship between steering angle $\theta_2$ and the parameters $u$, $v$, $l_1$, $\phi$. The partial derivatives of steering angle related to different variable parameters interpret the sensitivity of links to the output steering angle.

$$\begin{cases} \dfrac{\partial\theta_2}{\partial u} = \dfrac{-\cos(\theta_1+\phi)(x_E - x_C) + \sin(\theta_1+\phi)(y_E - y_C)}{l_1\sin(\psi-\theta_2)(x_E - x_C) - l_1\cos(\psi-\theta_2)(y_E - y_C)} \\ \dfrac{\partial\theta_2}{\partial v} = \dfrac{v}{l_1\sin(\psi-\theta_2)(x_E - x_C) - l_1\cos(\psi-\theta_2)(y_E - y_C)} \\ \dfrac{\partial\theta_2}{\partial l_1} = -\dfrac{[\cos(\psi+\theta_1) + \cos(\psi-\theta_2)](x_E - x_C) + [\sin(\psi-\theta_2) - \sin(\psi+\theta_1)](y_E - y_C)}{l_1\sin(\psi-\theta_2)(x_E - x_C) - l_1\cos(\psi-\theta_2)(y_E - y_C)} \\ \dfrac{\partial\theta_2}{\partial\phi} = \dfrac{u\sin(\theta_1+\phi)(x_E - x_C) + u\cos(\theta_1+\phi)(y_E - y_C)}{l_1\sin(\psi-\theta_2)(x_E - x_C) - l_1\cos(\psi-\theta_2)(y_E - y_C)} \end{cases} \quad (30)$$

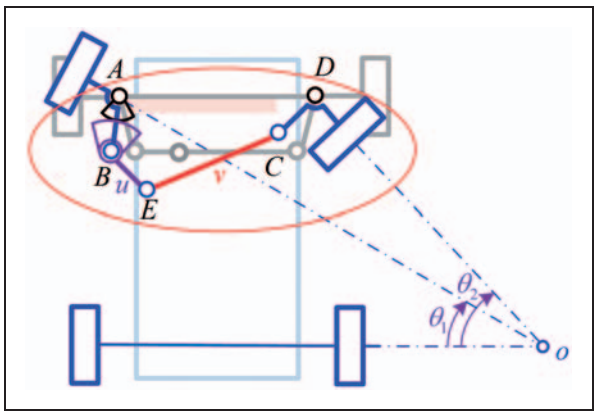


**Figure 4.** Geared steering mechanism to meet Ackermann turning geometry.

Therefore, combining with numerical simulation, the sensitivity values could be computed. Positive sensitivity values indicate that the output steering angle increases with the corresponding parameters and vice versa.

## Noncircular profile design

To facilitate the analysis of pitch curves of the noncircular incomplete gears, a local coordinate frame, $x_1o_1y_1$ shown in Figure 5, is established by letting the origin, $o_1$, be on the centre of gear 1 which is also the fixed revolute joint of link $AB$. The $x_1$-axis is along the link $AD$. The $y_1$-axis is pointing up. The coordinates of a point on the pitch curve can be expressed as

$$\begin{cases} x_1 = r_1\cos\varphi \\ y_1 = r_1\sin\varphi \end{cases} \quad (31)$$

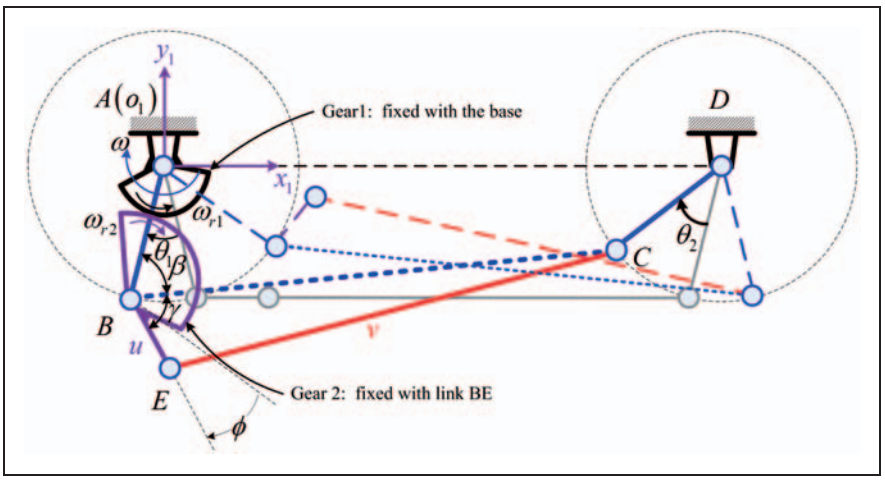


**Figure 5.** Geared five-bar steering mechanism.

where $\varphi$ represents the polar angle of point $P$ shown in Figure 6.

Specifying the parameters, $b$, $l$, $l_i(i = 1, 2, 4)$, $u$ and $v$, the pitch curve of the noncircular gear 1 can be obtained by associating equations (26) and (31). After knowing the pitch curves of the two noncircular incomplete gears, the addendum and dedendum curves can be obtained in line with the equidistance line formula. In the coordinate frame, $x_1o_1y_1$ shown in Figure 6, the addendum curve equation of the fixed noncircular incomplete gear can be represented by

$$\begin{cases} x_1^a = x_1 + \dfrac{\dfrac{dy_1}{d\varphi}}{\sqrt{\left(\dfrac{dx_1}{d\varphi}\right)^2 + \left(\dfrac{dy_1}{d\varphi}\right)^2}} h_a^* m \\ y_1^a = y_1 - \dfrac{\dfrac{dx_1}{d\varphi}}{\sqrt{\left(\dfrac{dx_1}{d\varphi}\right)^2 + \left(\dfrac{dy_1}{d\varphi}\right)^2}} h_a^* m \end{cases} \tag{32a}$$

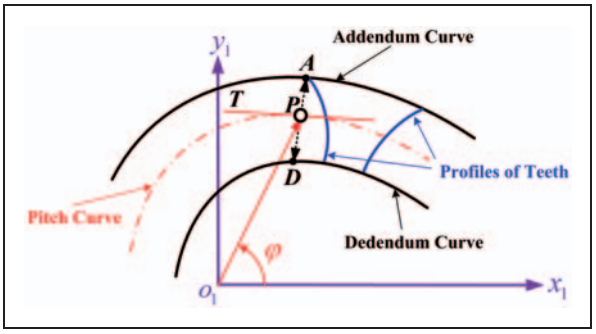


**Figure 6.** Addendum and dedendum curves of a noncircular incomplete gear.

where $x_1$ and $y_1$ are prescribed by equation (31), $h_a^*$ is the addendum coefficient, $m$ is the gear module, $\frac{dx_1}{d\varphi}$ is the derivative of $x_1$ with respect to $\varphi$, and $\frac{dy_1}{d\varphi}$ is the derivative of $y_1$ with respect to $\varphi$.

Similarly, the dedendum curve of the bottom noncircular gear can also be obtained as

$$\begin{cases} x_1^d = x_1 - \dfrac{\dfrac{dy_1}{d\varphi}}{\sqrt{\left(\dfrac{dx_1}{d\varphi}\right)^2 + \left(\dfrac{dy_1}{d\varphi}\right)^2}} h_f^* m \\ y_1^d = y_1 + \dfrac{\dfrac{dx_1}{d\varphi}}{\sqrt{\left(\dfrac{dx_1}{d\varphi}\right)^2 + \left(\dfrac{dy_1}{d\varphi}\right)^2}} h_f^* m \end{cases} \tag{32b}$$

where $h_f^*$ is the dedendum coefficient.

The functions of the addendum and dedendum curves are continuous because of the pitch curves are continuous as mentioned above.

For any point, $N$, on the gear profile shown in Figure 7, it either locates outside the pitch curve or inside (including on) it. Assume that the inward or outward normal of the profile on $N$ intersects the pitch curve at a point, $P$. The directional vectors, $r_1$, and its tangent line, $\boldsymbol{r}_1'$ will be

$$\begin{aligned} \boldsymbol{r}_1 &= \begin{bmatrix} r_1 \cos\varphi & r_1 \sin\varphi \end{bmatrix}^T, \\ \boldsymbol{r}_1' &= \begin{bmatrix} r_1' \cos\varphi - r_1 \sin\varphi & r_1' \sin\varphi + r_1 \cos\varphi \end{bmatrix}^T \end{aligned} \tag{33}$$

The tangent of the pitch curve at point $P$ is indicated by $PT$ in Figure 7, and the angle turned from $OP$ to $PT$ anticlockwise about point $P$ is denoted by $\mu \in (0, \pi)$.

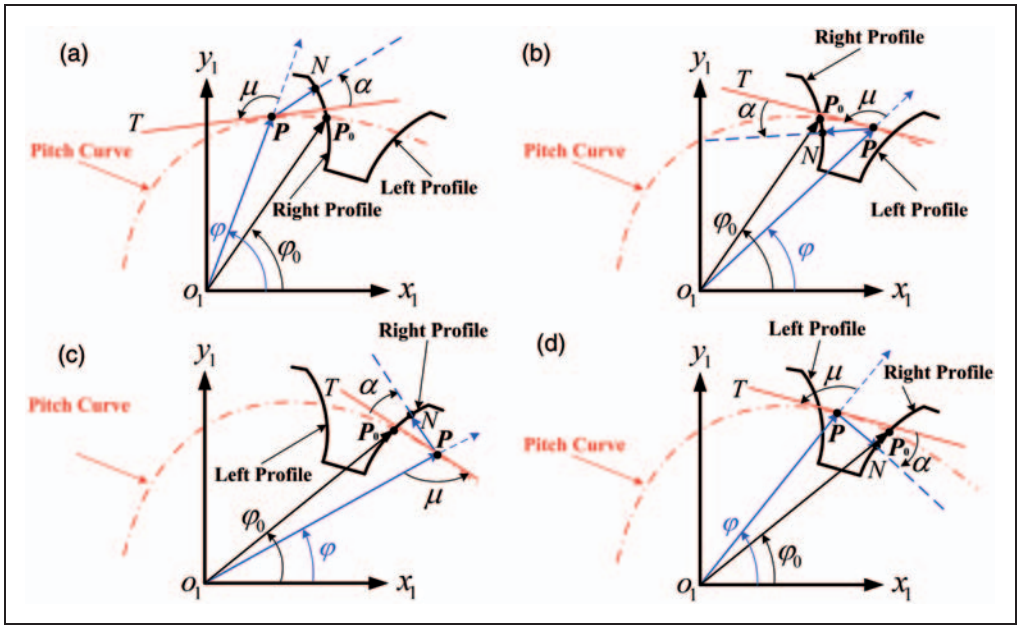


**Figure 7.** Tooth profiles of a noncircular incomplete gear.

Therefore

$$\cos\mu = \frac{\boldsymbol{r}_1 \cdot \boldsymbol{r}_1'}{||\boldsymbol{r}_1||\ ||\boldsymbol{r}_1'||} = \frac{r_1'(\varphi)}{\sqrt{r_1^2(\varphi) + \left[r_1'(\varphi)\right]^2}} \tag{34a}$$

where $\mu \in (0, \pi)$, $r_1(\varphi)$ is represented by equation (26), $r_1'(\varphi)$ is the derivative of $r_1(\varphi)$ with respect to $\varphi$, the polar angle of radial line $OP$. Alternatively, $\mu$ can also be expressed as

$$\tan\mu = \frac{r_1(\varphi)}{r_1'(\varphi)} \tag{34b}$$

The polar angle of vector $\overline{PN}$ shown in Figure 7(a) is

$$\psi_{Ro} = \varphi + \mu + \alpha - \pi \tag{35a}$$

where $\psi_{Ro}$ represents the polar angle of the vector $\overline{PN}$ when point $N$ locates on the right profile of the tooth and is outside of the pitch curve.

When point $N$ locates on the right profile of the tooth but is inside of the pitch curve shown in Figure 7(b), there is

$$\psi_{Ri} = \varphi + \mu + \alpha \tag{35b}$$

where $\psi_{Ri}$ represents the polar angle of the vector $\overline{PN}$ when point $N$ locates on the right profile of the tooth and is outside of the pitch curve.

Similarly, one can find that the polar angles of the vector $\overline{PN}$ when point $N$ locates on the left profile of the tooth, shown in Figure 7(c) and (d) are

$$\begin{cases} \psi_{Lo} = \varphi + \mu - \alpha \\ \psi_{Li} = \varphi + \mu - \alpha - \pi \end{cases} \tag{35c}$$

where $\psi_{Lo}$ represents the polar angle of the vector $\overline{PN}$ when point $N$ locates on the left profile of the tooth and is outside of the pitch curve, and $\psi_{Li}$ represents the polar angle of the vector $\overline{PN}$ when point $N$ locates on the left profile of the tooth and is outside of the pitch curve.

The coordinates of the profile can be expressed segment by segment as follows

$$\begin{cases} x_{1l} = r_1\cos\varphi \pm \int_{\varphi_0}^{\varphi} r_1(\varphi)\cos\alpha\cos(\varphi + \mu - \alpha)\mathrm{d}\varphi \\ y_{1l} = r_1\sin\varphi \pm \int_{\varphi_0}^{\varphi} r_1(\varphi)\cos\alpha\sin(\varphi + \mu - \alpha)\mathrm{d}\varphi \\ x_{1r} = r_1\cos\varphi \mp \int_{\varphi_0}^{\varphi} r_1(\varphi)\cos\alpha\cos(\varphi + \mu + \alpha)\mathrm{d}\varphi \\ y_{1r} = r_1\sin\varphi \mp \int_{\varphi_0}^{\varphi} r_1(\varphi)\cos\alpha\sin(\varphi + \mu + \alpha)\mathrm{d}\varphi \end{cases} \tag{36}$$

where the subscript $1l$ denotes the left profile of gear 1, subscript $1r$ denotes the right profile of gear 1, $r_1$ is the polar radius of point $P$ on gear 1, $\varphi_0$ is the polar angle of vector $\overline{o_1P_0}$ shown in Figure 7, the upper sign in $\pm$ or $\mp$ represents the profiles outside the pitch curve, while the lower sign represents the profiles inside the pitch curve, $P_0$ is the intersection points of the profiles and the pitch curve, $\mu \in (0, \pi)$ which can be worked out using equation (34), $\alpha$ is the specified pressure angle.

Theoretically, the profiles are defined precisely in accordance with equation (36); however, it is impossible to calculate the whole accurate points on the profiles. Therefore the calculation precision of the profiles depends on the interval of polar angle, $\varphi$, the smaller the interval is, the higher the precision will be.

For a standard spur gear, the pitch $p$ and the tooth thickness $s$ are both $\pi m/2$ on the pitch curve, where $m$ is the gear module. Therefore, the arc length determined by the two adjacent crossover points of the profiles and the pitch curve is $\pi m/2$. Then the polar angles of other intersection points, $\varphi_0$, can be determined by solving the integral equation

$$\int_0^{\varphi_0} r_{1L}(\varphi)\mathrm{d}\varphi = n\pi m/2 \tag{37}$$

For a rack cutter, the transitional curves are shaped by the envelope of the tip fillet of rack teeth. As shown in Figure 8, the rack cutter has tip fillets of identical radii of $\rho$. The points $S$ and $E$ represent the start point and end point of the fillet curve and $O_f$ is the centre of the fillet. Point $A$ is any point on the tip fillet. Line $AO_f$ and the pitch line intersect at point $C$. Since $O_f$ is the centre of the fillet, line $AO_f$, in fact, is the inward normal of the tip fillet. $\alpha_A$ is the acute angle subtended by $AC$ and the pitch line, so $\alpha < \alpha_A < \frac{\pi}{2}$ where $\alpha$ is the standard pressure angle. Consequently, there is

$$||\overrightarrow{CO_f}|| = \frac{h_{a_0}^* m - \rho\sin\alpha}{\sin\alpha_A} \tag{38}$$

where $||\overrightarrow{CO_f}||$ is the length of the line segment $CO_f$, $h_{a_0}^*$ is the addendum coefficient of the rack and generally equals 1, and $m$ is the module. Therefore

$$||\overrightarrow{AC}|| = ||\overrightarrow{CO_f}|| + \rho \tag{39}$$

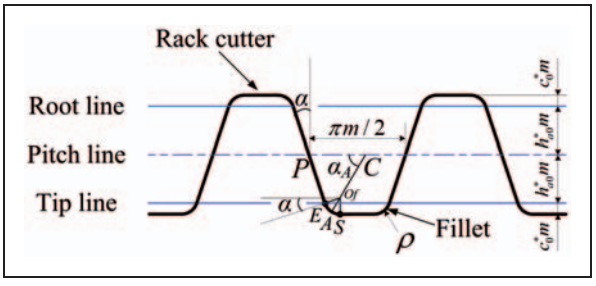


**Figure 8.** Rack cutter and tip fillet.

and

$$||\overrightarrow{CP}|| = h^*_{a0} m \tan\alpha + \rho\cos\alpha + ||\overrightarrow{CO_f}||\cos\alpha_A \tag{40}$$

where $||\overrightarrow{AC}||$ is the length of the line segment $AC$, and $\rho$ is the radius of the fillets shown in Figure 8.

Since line $AC$ is the inward normal of the tip fillet, the rack cutter tip fillet and the transition curve of the noncircular gear should be tangent at point $A$ if the pitch line of the rack cutter and the pitch curve of the noncircular gear are tangent at the point $C$. Therefore, the corresponding point on the transition curve can be determined when the position of point $A$ is specified.

Assume that the polar angle of $\overrightarrow{OC}$ is denoted by $\varphi_C$ and $\mu_C \in (0, \pi)$ is the subtended angle between the point vector and its tangent line at point $C$. Hence, $\varphi_C$ can be worked out using

$$\int_{\varphi_0}^{\varphi_C} r_{1L}(\varphi)d\varphi = ||\overrightarrow{CP}|| \tag{41}$$

where $\varphi_0$ is calculated by (37), and $||\overrightarrow{CP}||$ is represented with equation (40). Then $\mu_C$ can be worked out using (34) where $\varphi_{1L} = \varphi_C$.

Thus, after specifying the angle $\alpha_A$ shown in Figure 9, the polar angle of $\overrightarrow{CA}$ is

$$\varphi_{CA} = \varphi_C + \mu_C + \alpha_A - 2\pi \tag{42}$$

Therefore, the coordinates of the point $A$ are now represented by

$$\begin{cases} x_A = r_{1L}(\varphi_C)\cos\varphi_C + \left|\overrightarrow{AC}\right|\cos\varphi_{CA} \\ y_A = r_{1L}(\varphi_C)\sin\varphi_C + \left|\overrightarrow{AC}\right|\sin\varphi_{CA} \end{cases} \tag{43}$$

where $\varphi_C$ can be worked out using equation (41), and $\varphi_{CA}$ is represented by equation (42).

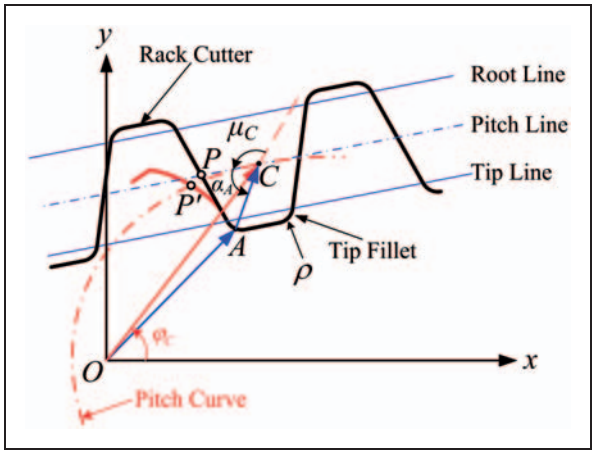


**Figure 9.** Coordinates of the transition curve.

When $\alpha_A$ changes from $\alpha$ to $\frac{\pi}{2}$, the position of point $A$ will correspondingly change on the tip fillet. To avoid undercutting by rack cutters, there should be

$$m_{\max} \leqslant \frac{\rho_{\min}\sin^2\alpha}{h^*_{a0}} \tag{44}$$

where $m_{\max}$ is the maximum gear module allowed, $\rho_{\min}$ is the minimal radius of curvature of the pitch curve, $h^*_{a0}$ is the addendum coefficient of the cutter and is generally equal to 1.

With theoretical analysis one can get the numerical method for gear profile as follows:

1. Substitute the structure parameters into equation (26) and get the pitch curves;
2. Calculate the addendum and dedendum curves in accordance with equation (32a) and (32b);
3. Calculate the maximum gear module allowed in accordance to equation (44), and choose an appropriate module $m$;
4. Assuming that the polar angle of the starting point $P_0$ on the pitch curve, $\varphi_0$, is specified and the corresponding profile is a right(left) profile;
5. Prescribe the interval of the polar angle $\varphi$, $\Delta\varphi$, such as $\Delta\varphi = 0.01rad$, then the polar angle of the $i$th$(i = 1, 2, 3, \ldots)$ point on the profile is $\varphi = \varphi_0 \pm i\Delta\varphi$;
6. Calculate the $\mu$ in line with equation (34b), then get the coordinates of the $i$th$(i = 1, 2, 3, \ldots)$ point on the profile according to equation (36);
7. Calculate the polar angle of the $i$th$(i = 1, 2, 3, \ldots)$ point $P_n$ on the pitch curve, $\varphi_n$, by solving the integral equation $\int_{\varphi_0}^{\varphi_n} r_1(\varphi)\mathrm{d}\varphi = n\pi m/2$;
8. Repeat steps 5–7 to complete the whole gear profile.

Moreover, the calculation precision of the pitch curves and the profiles respectively depend on the intervals of $\theta_1$ and $\varphi$.

## Parametric optimisation and numerical simulation

In general, the maximum turning angle allowed by front wheels is a certain value between $7\pi/36$ and $\pi/4$, and between 35° and 45° in degrees. For the steering mechanism shown in Figure 5, only the parameters $l_1$, $u$ and $\psi$ could be optimised because the structure parameters $b$, $l$ and $l_4$ are specified by the vehicle. To reach this target, the following process can be followed.

The steering mechanism should satisfy the request of the maximum turning angle of the front wheels which is not more than $\frac{\pi}{4}$. Consequently the maximum turning angle interval of the steering mechanism is $\theta_1 \in \left[\mathrm{arc\,cot}\left[\cot\left(-\frac{\pi}{4}\right) + \frac{b}{l}\right], \frac{\pi}{4}\right]$ in line with equation (10). Analysing the profile calculation method, one can find that the maximum polar angle $\theta_{1\max}$

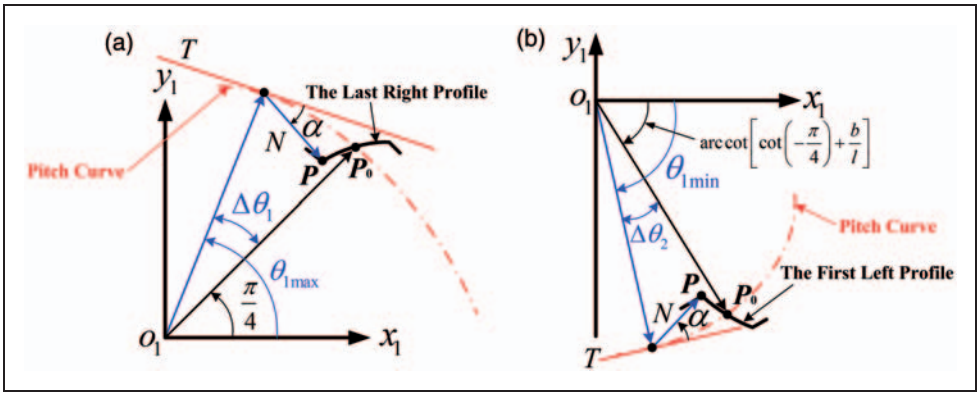


**Figure 10.** The extreme values of polar angle $\theta_1$.

should meet that $\theta_{1\max} > \frac{\pi}{4}$; otherwise it is impossible to get the last segment of the left profile, as shown in Figure 10(a). Similarly, the minimum polar angle $\theta_{1\min}$ should be smaller than the minimum turning angle which is represented in Figure 10(b). As a result, there should be $\theta_1 \in [\text{arc}\cot\left[\cot\left(-\frac{\pi}{4}\right)+\frac{b}{l}\right]-\Delta\theta_2, \frac{\pi}{4}+\Delta\theta_1]$ where $\Delta\theta_1$ and $\Delta\theta_2$ are determined by the pitch curves of the two gears.

Obviously, the coordinates of point $P$ satisfy both equation (32b) and equation (36). That is to say, one can obtain $\Delta\theta_1$ and $\Delta\theta_2$ by associating equation (32b) and equation (36). Generally, it is safe to assume $\Delta\theta_1 = \Delta\theta_2 = 10^\circ$. For instance, assuming that $b = 1600\,\text{mm}$, $l = 2800\,\text{mm}$; then $\theta_1 \in [-76.8^\circ, 55^\circ]$.

What follows will investigate the optimisation of the structure parameters of the steering mechanism.

### The optimisation variables and constraint conditions

As mentioned above, the optimisation variables, in vector form, can be expressed as

$$\boldsymbol{x} = \begin{bmatrix} l_1 & u & \psi \end{bmatrix}^T \tag{45}$$

Firstly, the parameters should be neither too big nor too small so long as they meet the space arrangement of chassis. The upper and lower limits of the variable vectors can be expressed with

$$\begin{cases} \boldsymbol{x}_U = \begin{bmatrix} l_{1\max} & u_{\max} & \psi_{\max} \end{bmatrix}^T \\ \boldsymbol{x}_L = \begin{bmatrix} l_{1\min} & u_{\min} & \psi_{\min} \end{bmatrix}^T \end{cases} \tag{46}$$

The minimum radius of pitch curves should not be too small, otherwise structure interference might occur. Assume that the minimum radius of pitch curve of gear 1 is $\rho_1$ and the minimum radius of pitch curve of gear 2 is $\rho_2$. Associating equation (26) presents

$$\begin{cases} r_1 = -\dfrac{i_{21}^r(\boldsymbol{x}) l_1}{1 - i_{21}^r(\boldsymbol{x})} \geqslant \rho_1 \\ r_2 = \dfrac{l_1}{1 - i_{21}^r(\boldsymbol{x})} \geqslant \rho_2 \end{cases} \tag{47}$$

**Table 1.** Primary parameters of a vehicle.

| Sequence | $l_4$ (mm) | $l$ (mm) | $b$ (mm) | $m$ (mm) | $\alpha$ (°) | $h_a^*$ | $h_f^*$ |
|---|---|---|---|---|---|---|---|
| 1 | 1200 | 2800 | 1600 | 2 | 20 | 1 | 1.25 |
| 2 | 1350 | 2800 | 1600 | 2 | 20 | 1 | 1.25 |
| 3 | 1350 | 2950 | 1600 | 2 | 20 | 1 | 1.25 |
| 4 | 1350 | 2950 | 1750 | 2 | 20 | 1 | 1.25 |

**Table 2.** Optimisation results.

| Sequence | $l_1$ (mm) | $u$ (mm) | $\psi$ (rad) |
|---|---|---|---|
| 1 | 100.00 | 26.24 | $\frac{7\pi}{12}$ |
| 2 | 100.00 | 26.24 | $\frac{7\pi}{12}$ |
| 3 | 100.00 | 25.96 | $\frac{7\pi}{12}$ |
| 4 | 100.00 | 26.42 | $\frac{7\pi}{12}$ |

As a result, the transmission ratio satisfies that

$$\frac{\rho_1}{l_1 - \rho_1} \leqslant -i_{21}^r(\boldsymbol{x}) \leqslant \frac{l_1 - \rho_2}{\rho_2} \tag{48}$$

Inequality (48) always holds for $\theta_1 \in [\theta_{1\min}, \theta_{1\max}]$.

### Object function and the optimisation analysis

The particular characteristic of noncircular gear is that the transmission ratio is variable within a certain interval. To keep a balanced design for a pair of meshing noncircular, the width of the interval should be as narrow as possible. Suppose

$$E(\boldsymbol{x}) = \frac{\int_{\theta_{1\min}}^{\theta_{1\max}} i_{21}^r(\theta_1, \boldsymbol{x})\mathrm{d}\theta_1}{\theta_{1\max} - \theta_{1\min}} = \frac{\phi(\theta_{1\max}, \boldsymbol{x}) - \phi(\theta_{1\min}, \boldsymbol{x})}{\theta_{1\max} - \theta_{1\min}} \tag{49}$$

where $E(\boldsymbol{x})$ denotes the mean value of $i_{21}^r(\theta_1, \boldsymbol{x})$ within the interval $[\theta_{1\min}, \theta_{1\max}]$.

The variance of transmission ratio can be subsequently defined as

$$f(\boldsymbol{x}) = \frac{\int_{\theta_{1\min}}^{\theta_{1\max}} \left[i_{21}^{r}(\theta_1, \boldsymbol{x}) - E(\boldsymbol{x})\right]^2 \mathrm{d}\theta_1}{\theta_{1\max} - \theta_{1\min}} \tag{50}$$

Substituting the equation (49) to equation (50) and simplifying it presents

$$f(\boldsymbol{x}) = \frac{\int_{\theta_{1\min}}^{\theta_{1\max}} \left[i_{21}^{r}(\theta_1, \boldsymbol{x})\right]^2 \mathrm{d}\theta_1}{\theta_{1\max} - \theta_{1\min}} - E(\boldsymbol{x})^2 \tag{51}$$

where $f(\boldsymbol{x})$ measures the variable amplitude of the transmission ratio. Thus the object function, $F(\boldsymbol{x})$, can be defined as

$$F(\boldsymbol{x}) = \min[f(\boldsymbol{x})] \tag{52}$$

where $\boldsymbol{x}$ is subjected to inequality (48) while $\boldsymbol{x}_L \leqslant \boldsymbol{x} \leqslant \boldsymbol{x}_U$.

Because $i_{21}^{r}(\boldsymbol{x})$ and $\phi(\boldsymbol{x})$ are continuous functions about $\boldsymbol{x}$, so $f(\boldsymbol{x})$ is also a continuous function. As a result, the minimum value of $f(\boldsymbol{x})$ must occur at one of the three points, the upper boundary of the $\boldsymbol{x}$-variable interval, the lower boundary of the $\boldsymbol{x}$-variable interval and the point where the partial derivative of $f(\boldsymbol{x})$ with respect to $\boldsymbol{x}$ equals zero. The partial derivative of $f(\boldsymbol{x})$ can be expressed as

$$\frac{\partial f(\boldsymbol{x})}{\partial \boldsymbol{x}} = \frac{2\left\{\int_{\theta_{1\min}}^{\theta_{1\max}} i_{21}^{r}(\theta_1, \boldsymbol{x}) \dfrac{\partial i_{21}^{r}(\theta_1, \boldsymbol{x})}{\partial \boldsymbol{x}} \mathrm{d}\theta_1 - [\phi(\theta_{1\max}, \boldsymbol{x}) - \phi(\theta_{1\min}, \boldsymbol{x})] \dfrac{\partial E(\boldsymbol{x})}{\partial \boldsymbol{x}}\right\}}{\theta_{1\max} - \theta_{1\min}} \tag{53}$$

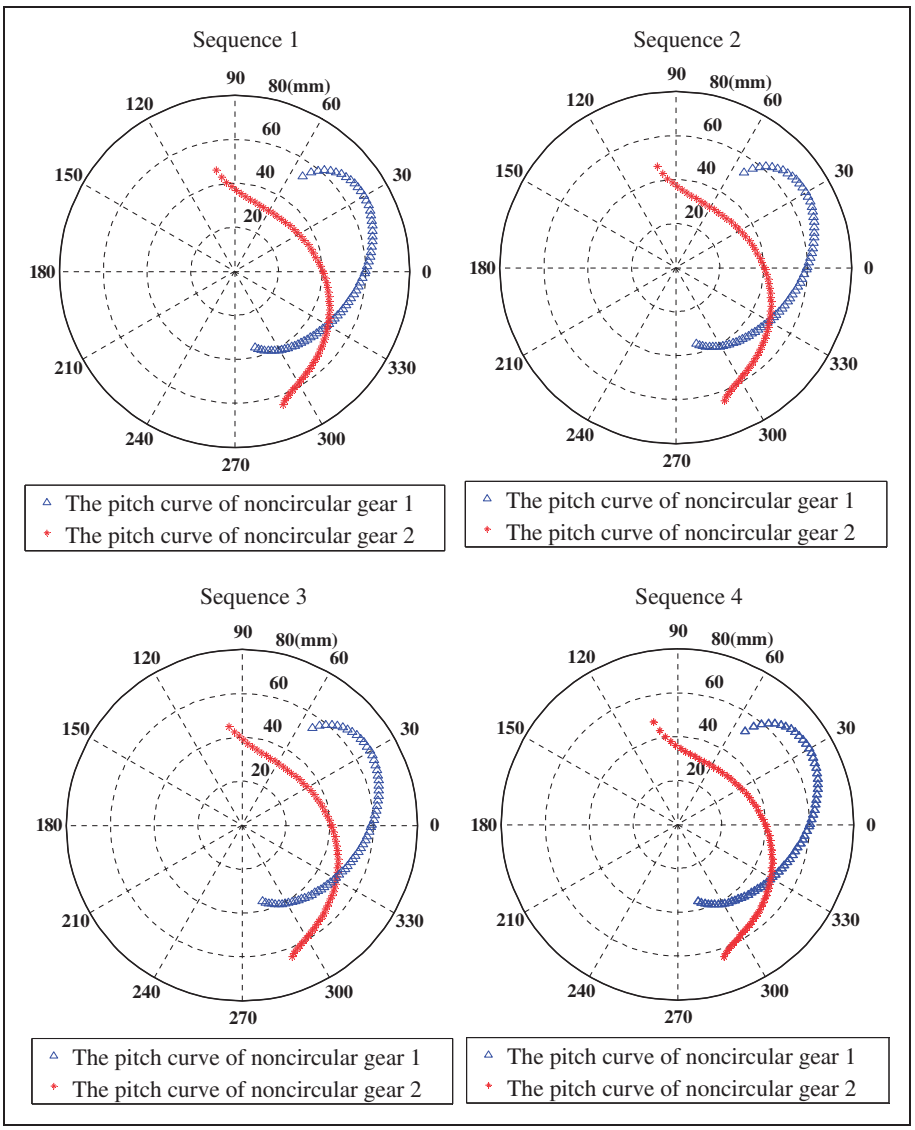


**Figure 11.** The pitch curves of noncircular gears in polar coordinate.

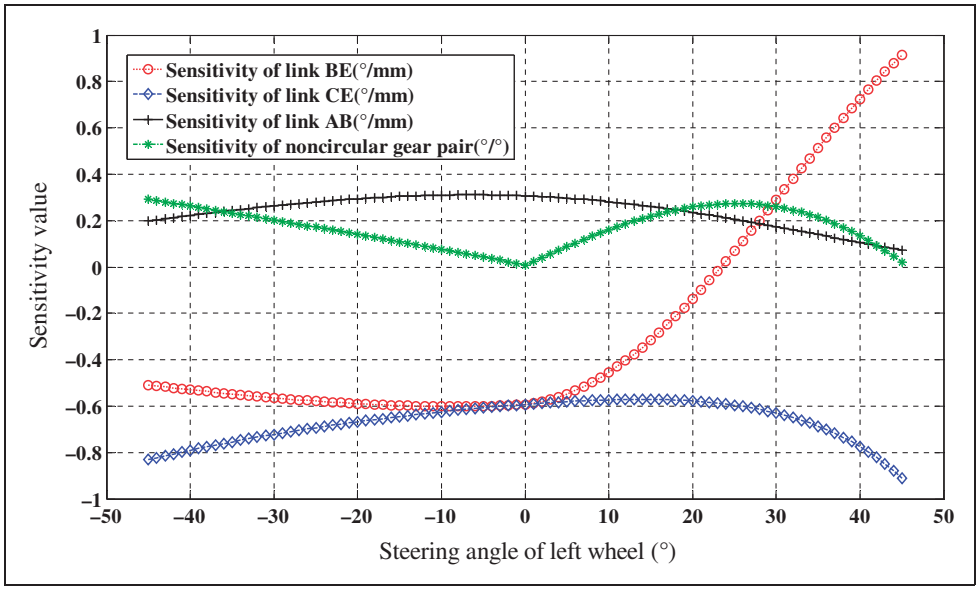


**Figure 12.** Sensitivity values with parameters in sequence 1.

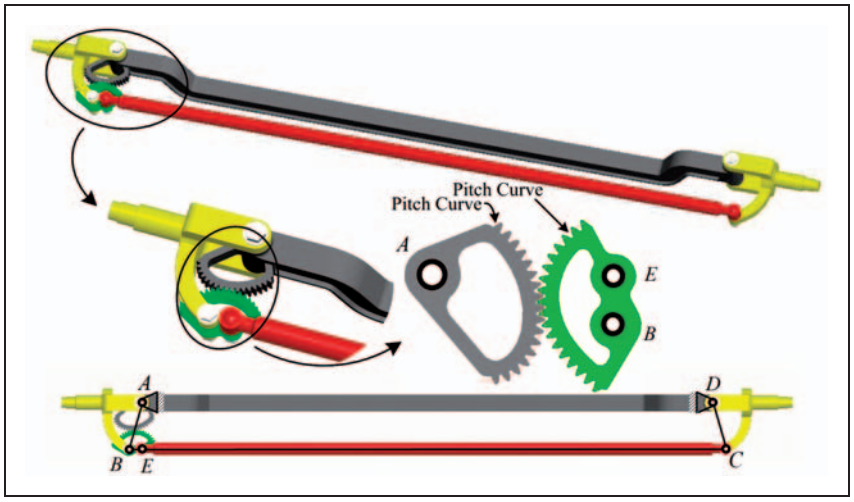


**Figure 13.** Assembly of an Ackermann-type steering mechanism.

The numerical algorithm such as trapezoid integration formula can be used to obtain an enough precise solution of the above problem by programming at MATLAB. The program is not discussed here for the sake of length.

Listed in Table 1 are the primary parameters of a vehicle. With these parameters, numerical simulations based on the optimisation method proposed above are executed. Suppose that

$$\begin{cases} \boldsymbol{x}_U = \begin{bmatrix} 200 & 80 & 75^\circ \end{bmatrix}^T \\ \boldsymbol{x}_L = \begin{bmatrix} 100 & 20 & 105^\circ \end{bmatrix}^T \end{cases}, \quad \rho_1 = \rho_2 = 20\,\text{mm}$$

Four sets of vehicle parameters shown in Table 1 are used to demonstrate the effectiveness of the method. The optimisation results are listed in Table 2.

The pitch curves of noncircular gears corresponding to the parameters listed in Tables 1 and 2 in polar coordinate are presented in Figure 11. And the gear profile can be obtained by numerical method aforementioned.

Accordingly, the sensitivity values can be computed, as Figure 12 shows, by substituting the parameters in sequence 1 into equation (30). From Figure 12 one can find that the variation range of the sensitivity value of link $BE$ is the largest, but the absolute sensitivity value of link $CE$ is the largest. Therefore, the wear resistance ability of joints connected to link $BE$ and $CE$ should be improved in applications, or the joints with preload function can be used in this system to reduce the influence of wear in joints. What's more, the steering system design should allow the vehicle to tend to under-steer once the abrasion occurs.

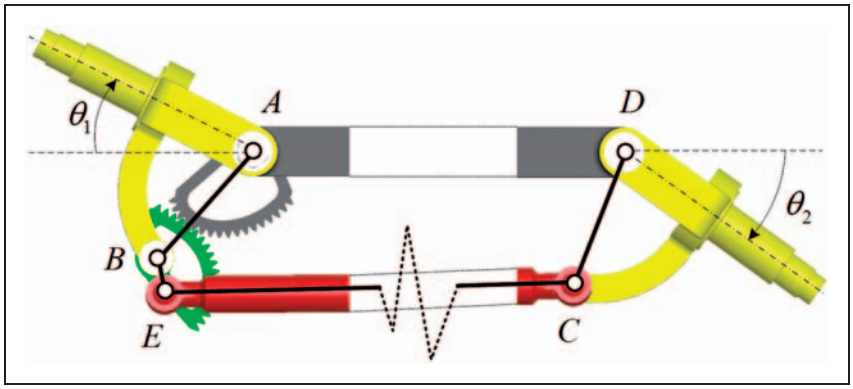


**Figure 14.** Steering motion of the mechanism.

With any set of parameters of Tables 1 and 2, the first set of parameters for example, an Ackermann-type steering mechanism can be designed and assembled by software Pro/Engineer 4.0 as shown in Figure 13.

Figure 13 indicates that this kind of steering mechanism is similar in structural compactness to the trapezoid four-bar mechanism but can precisely satisfy the Ackermann turning requirements. And the steering motion of the proposed mechanism is verified in Figure 14. In applications, the pitch curve might be modified when taking account of the tires and other elastic elements. However, the method proposed in this article can be used to design an ideal Ackermann-type steering mechanism.

## Conclusions

This article proposed a steering mechanism that precisely satisfies the needs of Ackermann turning geometry. After pointing out that a planar four-bar linkage could exactly trace 9 points at most, it put the Ackermann criteria into the size synthesis for steering mechanism by using the incomplete noncircular gears. Therefore, the synthesis of the steering mechanism become the design of the pitch curves, addendum curves, dedendum curves, tooth profiles and transition curves of a pair of noncircular gears. Kinematic simulations shown that the target of design could be completely reached by the incomplete noncircular gear coupled five-link mechanism. The steering mechanism should improve the vehicle steering performance but has similar structure to the existing steering four-bar linkages; as a result, it has a very wide application prospect especially in the light carriages.

### Funding

This research was supported by the Natural Science Foundation of Beijing under Grant 3112014, the National Natural Science Foundation of China under Grant 51175277 and the Program for New Century Excellent Talents in University. The authors gratefully acknowledge these support agencies.

### References

1. Pramanik S. Kinematic synthesis of a six-member mechanism for automotive steering. *J Mech Des* 2002; 124(4): 642–645.
2. Reimpell H, Stoll H and Betzler JW. *The automotive chassis: engineering principles*. 2nd edn. Oxford: Butterworth Heinemann, 2002.
3. Suh CH and Mecklenburg AW. Optimal design of mechanisms with the use of matrices and least squares. *Mech Mach Theory* 1973; 8: 479–495.
4. Simionescu PA and Beale D. Optimum synthesis of the four-bar function generator in its symmetric embodiment: the Ackermann steering linkage. *Mech Mach Theory* 2002; 37(12): 1487–1504.
5. Simionescu PA and Talpasanu I. Synthesis and analysis of the steering system of an adjustable tread-width four-wheel tractor. *Mech Mach Theory* 2007; 42(5): 526–540.
6. Simionescu PA, Beale D and Talpasanu I. Dynamic effect of the bump steer in a wheeled tractor. *Mech Mach Theory* 2007; 42(10): 1352–1361.
7. Simionescu PA and Smith MR. Initial estimates in the design of central-lever steering linkages. *J Mech Des* 2002; 124(4): 646–651.
8. Zarak CE and Townsend MA. Optimal design of rack-and-pinion steering linkages. *J Mech Trans Auto Des* 1983; 105(2): 220–226.
9. Erdman AG, Sandor GN and Kota S. *Mechanism design: analysis and synthesis*. Englewood Cliffs, NJ: Prentice Hall, 2001.
10. Rahmani Hanzaki A, Rao PVM and Saha SK. Kinematic and sensitivity analysis and optimization of planar rack-and-pinion steering linkages. *Mech Mach Theory* 2009; 44(1): 42–56.
11. Chicurel E. A steering interval mechanism. *Mech Mach Theory* 1999; 34(3): 421–436.
12. David DA and Danwen Q. Analytical design of seven joint spatial steering mechanisms. *Mech Mach Theory* 1987; 22(4): 315–319.
13. Simionescu PA, Smith MR and Tempea I. Synthesis and analysis of the two loop translational input steering mechanism. *Mech Mach Theory* 2000; 35(7): 927–943.
14. Simionescu PA and Smith MR. Applications of watt II function generator cognates. *Mech Mach Theory* 2000; 35(11): 1535–1549.
15. Felzien ML and Cronin DL. Steering error optimization of the Macpherson strut automotive front suspension. *Mech Mach Theory* 1985; 20(1): 17–26.

16. Mántaras DA, Pablo L and Carlos V. Development and validation of a three-dimensional kinematic model for the McPherson steering and suspension mechanisms. *Mech Mach Theory* 2004; 39(6): 603–619.
17. Antonio C and Walter D'A. A function generating differential mechanism for an exact solution of the steering problem. *Mech Mach Theory* 1998; 33(5): 535–549.
18. Raghavan M. Number and dimensional synthesis of independent suspension mechanisms. *Mech Mach Theory* 1996; 31(8): 999–1195.
19. Huang XZ and Zhang YM. Reliability sensitivity analysis for rack-and-pinion steering linkages. *J Mech Des* 2010; 132(7): 071012.
20. Emura T and Arakawa A. A new steering mechanism using noncircular gears. *JSME Int J* 1992; 35(4): 604–610.
21. Donner DB. Function generation utilizing an eight-link mechanism and optimized non-circular gear elements with application to automotive steering. *Proc IMechE, Part C: J Mechanical Engineering Science* 2001; 215(7): 847–857.
22. Miller G, Reed R and Wheeler F. Optimum Ackerman for improved steering axle tire wear on trucks. SAE Technical Paper, No. 912693.
23. Hunt KH. *Kinematic geometry of mechanisms*. Oxford: Oxford University Press, 1978.

## Appendix

### Notation

| | |
|---|---|
| $b$ | track of front wheels (mm) |
| $h_a^*$ | addendum coefficient |
| $h_f^*$ | dedendum coefficient |
| $i_{21}^r$ | relative transmission ratio of the noncircular gear 1 and gear 2 |
| $l$ | wheel base (mm) |
| $l_1$ | length of swing arm of the trapezoid linkage (mm) |
| $l_2$ | length of link $BC$ that satisfies Ackermann criteria (mm) |
| $l_{20}$ | length of link $BC$ when turning angle equals to zero (mm) |
| $l_4$ | length of link $AD$ (mm) |
| $m$ | gear module |
| $m_{\max}$ | maximum gear module allowed |
| $p$ | pitch (mm) |
| $r_1$ | radius of noncircular gear 1 (mm) |
| $r_2$ | radius of noncircular gear 2 (mm) |
| $s_i (i = 1, 2, 3, 4, 5, 6)$ | length of each link shown in Figure 2 (mm) |
| $u$ | length of link $BE$ (mm) |
| $v$ | length of link $EC$ (mm) |
| $\alpha$ | pressure angle (°) |
| $\alpha_A$ | acute angle subtended shown in Figure 8 (rad) |
| $\beta$ | angle between link $AB$ and $BC$ (rad) |
| $\Delta\varphi$ | interval of the polar angle (rad) |
| $\gamma$ | angle between link $BC$ and $BE$ (rad) |
| $\mu$ | angle turned from $OP$ to $PT$ anticlockwise about point $P$ (rad) |
| $\mu_C$ | subtended angle between the point vector and its tangent line at point $C$ (rad) |
| $\omega$ | angular velocity of link $AB$ (rad/s) |
| $\omega_{r1}$ | relative angular velocity of noncircular gear 1 with respect to link $AB$ (rad/s) |
| $\omega_{r2}$ | relative angular velocity of noncircular gear 2 with respect to link $AB$ (rad/s) |
| $\phi$ | relative rotational angle between $\overrightarrow{BA}$ and $\overrightarrow{BE}$ (rad) |
| $\varphi$ | polar angle of point $P$ shown in Figure 6 (rad) |
| $\varphi_C$ | polar angle of $\overrightarrow{OC}$ shown in Figure 9 (rad) |
| $\varphi_i (i = 1, 2)$ | input and output angles of a four-bar linkage (rad) |
| $\psi$ | bottom angle of a trapezoid linkage (rad) |
| $\rho$ | radius of the fillets shown in Figure 8 (mm) |
| $\rho_1$ | minimum radius of pitch curve of noncircular gear 1 (mm) |
| $\rho_2$ | minimum radius of pitch curve of noncircular gear 2 (mm) |
| $\rho_{\min}$ | minimal radius of curvature of the pitch curve |
| $\theta$ | subtended angle shown in Figure 2 (rad) |
| $\theta_1$ | steering angle of the front left wheel (rad) |
| $\theta_2$ | steering angle of the front left wheel (rad) |
| $\xi$ | $\xi = \frac{l_1}{l_4}$ |
| $\zeta$ | $\varsigma = \frac{b}{l}$ |